We are IntechOpen, the world's leading publisher of Open Access books Built by scientists, for scientists

6,900
Open access books available

185,000
International authors and editors

200M
Downloads

Our authors are among the

154
Countries delivered to

TOP 1%
most cited scientists

12.2%
Contributors from top 500 universities



WEB OF SCIENCE™

Selection of our books indexed in the Book Citation Index in Web of Science™ Core Collection (BKCI)

Interested in publishing with us?
Contact book.department@intechopen.com

Numbers displayed above are based on latest data collected.
For more information visit www.intechopen.com



15

Future Uses of Three/Four Dimensional Power Doppler Signal in Fetal Medicine

Juan Carlos Bello-Munoz[1], Mauricio Ayala[2],
Elena Carreras[1], Paula Oliveros[1], Nazareth Campo[1],
Alexandra Casasbuenas[1], Silvia Arévalo[1] and Lluis Cabero[1]
[1]*Department of Obstetrics, Vall d'Hebron University Hospital; Universitat Autónoma de Barcelona; Catalonia*
[2]*Department of Applied Physics and Mathematics; Universitat Autónoma de Barcelona; Catalonia*
Spain

1. Introduction

Three-dimensional Ultrasound (3DUS) has grown quickly and constantly over the last fifteen years. However, some of its best clinical uses remain to be defined. The three-dimensional Power Doppler (PD) is based on the ability to register the signal amplitude of the ultrasound wave, which allows us to depict most moving particles in a given Region of Interest (ROI). It is also based on the three-dimensional US principles, that permit the collection of signals from such particles in a given Volume of Interest (VOI) The inclusion of a time sequencing protocol or a Space-Time Image correlation (STIC) algorithm, developed and made available to last generation US machines, adds the additional possibility of following the signal evolution during a pre-established lap. At first, this promising tool was used to evaluate vascularisation and perfusion in a series of foetal organs, finding neither adequate accuracy nor repeatability. Nowadays, its use in Foetal Medicine is restricted to certain foetal conditions, although new research is on-going and further uses for this technology are being unveiled.

As is it largely understood (Burns 1992), there are compelling scientific and medical reasons to seek measuring the volumetric flow rate, which means to estimate the volume of flow delivered per minute to a tissue bed. No doubt, the success in delivering oxygen and nutrients to the tissues depends, mainly, on the amount of blood delivered to such tissues per unit of time. At the beginning of the Doppler ultrasound era, a number of attempts to achieve this calculation were done (Gill 1979; Eik-Nes et al. 1982; Sauders et al. 1980). The standard method for estimating volume flow using sonography consists on multiplying the mean spatial velocity by the luminal cross-sectional area. However, it is well known that this technique has many problems; these include the inherent variability of vessel geometry, inaccurate assumptions about flow profile, B-dimensional sampling, and other important technical limitations derived from the way pulsed and spectral Doppler signals are registered, not to mention an unsustainable amount of human interaction in the final

estimation (J M Rubin 1999). All of the abovementioned reasons caused those efforts to fail and led this pretension to be forsaken for two decades.

Then, the experimental analysis of the Doppler Effect was described – taking into account the amplitude of the wave and tracking the acoustic speckle pattern produced by the echoes from moving blood (J M Rubin et al. 1994; Forsberg et al. 1995; Harrington et al. 1996; J M Rubin 1999). From those initial approaches, the concept of Fractional Moving Blood Volume (FMBV) (J M Rubin et al. 1997) was developed, which was mainly a mathematical normalization process of the colour pattern obtained from the power Doppler signal acquisition (Tomas Jansson et al. 2003; A. Welsh 2004). Preliminary publications established a direct relationship between the data from FMBV acquired by registering the power Doppler signal in a given Region of Interest (ROI) and actual perfusion of the tissue as measured by invasive methods in animal models (E Hernandez-Andrade, T Jansson, et al. 2004; E Hernandez-Andrade, Thuring-Jönsson, et al. 2004). It has been recently described how, under certain foetal conditions such as foetal growth restriction, some perfusion patterns are objectively altered and significantly differ from "normal" patterns established by the authors (E Hernandez-Andrade et al. 2008; Rogelio Cruz-Martinez et al. 2009; R Cruz-Martinez et al. 2011).

Nonetheless, there are still enormous gaps between the information obtained by FMBV and the actual estimations of, either, flow or perfusion (A. Welsh 2004; Lai et al. 2010). There are some boundaries which will limit insurmountably the utility of this technique, such as the low repeatability when comparing one patient with the same in a better acquisition setting - or one patient with difficulties for exploration like obese or anxious mothers to a normal one. Additionally, it will be impossible to relate such magnitudes with flow whenever there is no time frame considered in the image quantification process (A. W. Welsh et al. 2005).

No additional experience in this technique has been published and very likely it will not in the future. The next logical step would be to evaluate the possibilities of three dimensional ultrasound and power Doppler as an alternative approach to this phenomenon.

2. Three-dimensional power Doppler signal and the vascular indexes

Three-dimensional power Doppler (PD) became available for medical purposes towards the end of the last century (Fenster, Lee, et al. 1998; Guo, Durand, et al. 1998). It exhibited some advantages, considering the higher sensitivity of the PD for detecting, and therefore depicting, moving particles. Its first clinical application was designed to evaluate vascularisation in compromised regions, trying to elucidate whether there was an obstruction or not in a given vessel (Guo & Fenster 1996). Considering its potential for depicting vascular structure accurately, it was employed as a tool for measuring potentially angiogenic structures as tumours (Bendick et al. 1998; Kupesic & Kurjak 2000). Also its potential for depicting vascular architecture and potential anomalies has been considered as promising (Fig. 1) (Heling, Chaoui, et al. 2000; Chaoui & Kalache 2001)

Nevertheless, the information given by this technique was rather limited, considering there was no quantification of the signal and no objective measurements would be done. Then, a mathematical algorithm was developed, firstly used in gynaecology (J M Rubin 1999; Pairleitner et al. 1999); based on the possibility of a direct correlation between PD signal

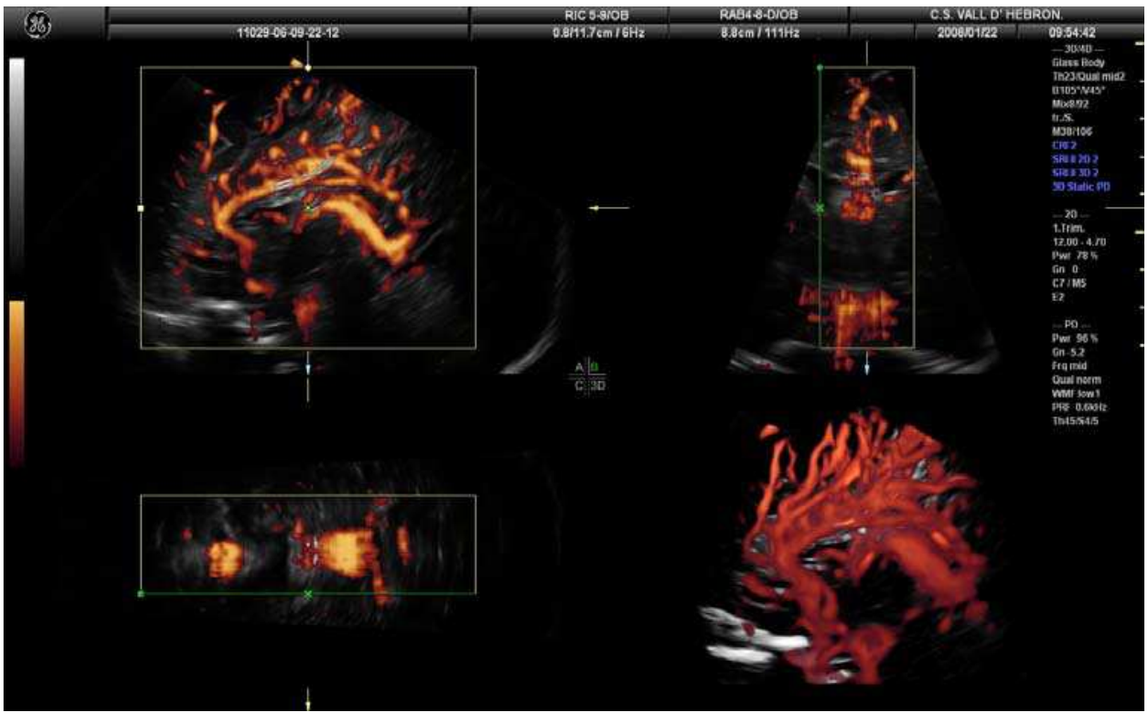


Fig. 1. Three dimensional PD angio mode rendering of intracranial blood vascularisation in a term fetus

intensity and, somehow, the velocity of the particles and the possible quantification of moving particles in a Volume of Interest (VOI) over the amount of grayscale, B-mode, particles in the same VOI. Three indexes were developed, which could indirectly give a mathematical expression of vascularisation and flow:

*Vascularization index (VI) = color voxels/(total voxels − background voxels)

$$VI = \frac{\sum_{c=1}^{100} hc(c)}{\sum_{g=1}^{100} hg(g) + \sum_{c=1}^{100} hc(c)} \tag{1}$$

Where
g= gray-scale value in the US image, normalized to 0-100: lowest intensity= 1; highest = 100
c= color value in the US image from power Doppler signal representation. Normalized to 0-100: lowest intensity= 1; highest = 100
hg(x) = frequency of gray-value x in US image
hc(x) = frequency of color value x in US image
*Flow index (FI) = weighted color voxels/color voxels

$$FI = \frac{\sum_{c=1}^{100} c \cdot hc(c)}{\sum_{c=1}^{100} hc(c)} \tag{2}$$

*Vascularization–flow index 1 (VFI) = weighted color voxels/(total voxels - background voxels)

$$VFI = \frac{\sum_{c=1}^{100} c \cdot hc(c)}{\sum_{g=1}^{100} hg(g) + \sum_{c=1}^{100} hc(c)} \tag{3}$$

Based on the above mentioned indexes, a number of research communications have been produced, evaluating the vascularity of benign versus malign ovarian masses (Kurjak et al. 1998; Juan Luis Alcázar & Jurado 2011) and prostatic tumours (Moskalik et al. 2001). Regarding the feto-placental unit, several attempts to correlate those indexes with regional perfusion of foetal brain (Hayashi et al. 1998; Nardozza et al. 2009), liver (C.-H. Chang et al. 2003), and lungs in normal (Dubiel et al. 2005) as well as pathologic *in-utero* conditions (Ruano et al. 2006). However, the clinical efficacy of this method remains unsupported by the evidence. No clinical findings can be drawn from those values so far. (Fig. 2)

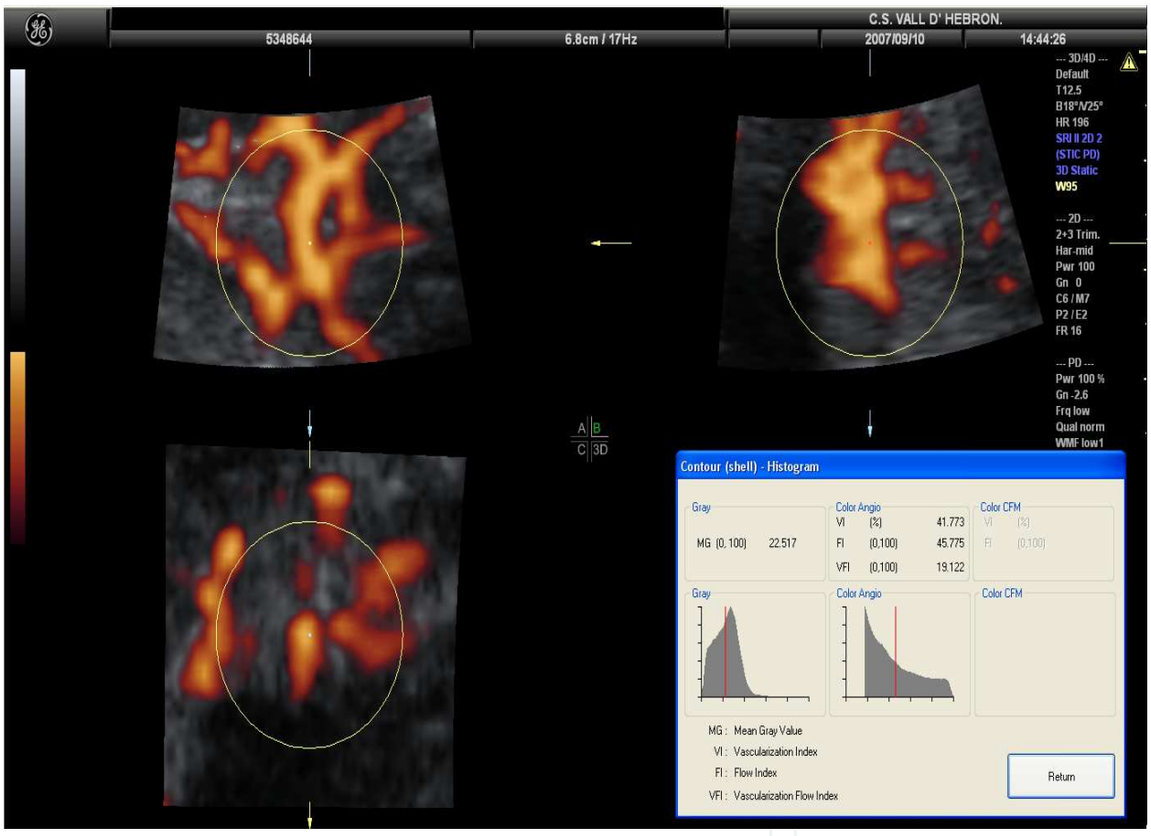


Fig. 2. Three dimensional PD angio mode rendering of intracranial blood vascularisation in a mid-trimester foetus with suspected brain sparing. In the right lower corner it is possible to visualize the histogram with the indexes obtained from the spherical shape –Volume of Interest

A promising field, still open to research, is the analysis of placental vasculature and its potential relationship to placental dysfunction (N. W. Jones et al. 2011). Some authors have found a positive correlation between low vascularisation indexes in early pregnancy and Fetal Growth Restriction (FGR) (Bozkurt, Başgül Yigiter, et al. 2010; Dar et al. 2010; Guimarães Filho et al. 2011; Morel et al. 2010; Negrini et al. 2011; A. O. Odibo et al. 2011;

Pomorski et al. 2011; Rizzo et al. 2009). It seems that the evaluation of first trimester placental vascularisation correlates, somehow, with a compromised placentation and therefore could predict some adverse perinatal outcomes of placental origin. Besides, the technique exhibits fairly good repeatability and accuracy (Tuuli et al. 2010; Martins & N J Raine-Fenning 2010; Yigiter et al. 2011).

The challenges for the future involve overcoming some of the technical problems that the three dimensional PD is plagued with and also to establish an adequate normalisation protocol, which it is currently lacking. (Fig. 3)

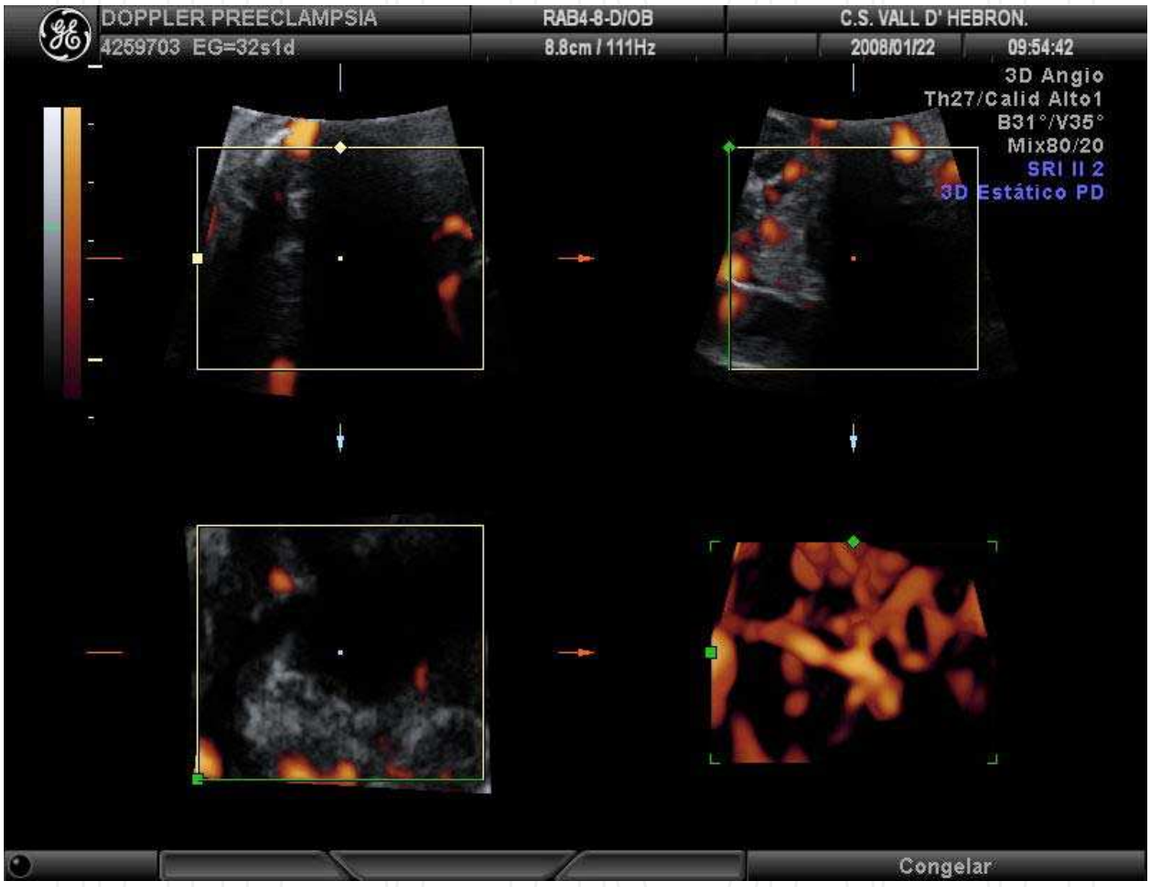


Fig. 3. Three dimensional angio mode rendering of placental vascularisation in a pre-eclampsia patient. Quantification of vascular branches suggests a lower flow in the corial plate when compared to volumes taken at the same gestational age from normal gestations

Another recently attempted and straightforward approach is to use 3D PD for the evaluation of progressive foetal conditions such as foetal goitrous hypothyroidism (Marín et al. 2010): In a given patient, under well-controlled conditions, it should be possible to evaluate the progression of either, an inflammatory response or the success of the treatment, which was thyroid hormone supplementation in that case. (Fig. 4).

Despite being rather promising, the 3D PD still has important limitations, some related to the power Doppler signal itself and some derived from acoustic impedance and mechanical interference. Some of these aspects are going to be discussed further in the next section.

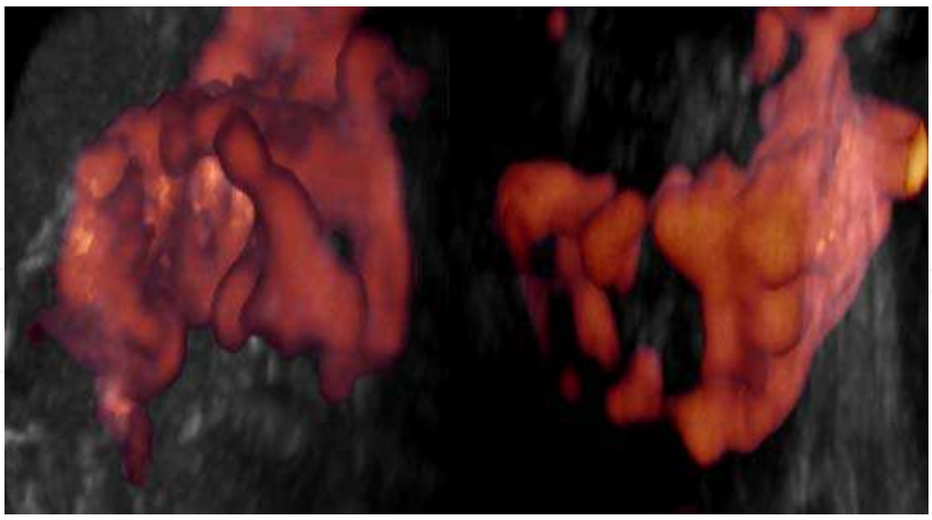


Fig. 4. Three dimensional PD angio mode rendered image of Thyroid gland of the same human foetus, before (left side) and after four weeks of intra-amniotic thyroid hormone supplementation (right side). Actual volume of the gland changed according to foetal growth, but vascularisation decreased markedly after treatment

2.1 The signal normalization problem and its consequences

To normalize the 3D PD signal, it is necessary to take into account three paramount boundaries:

- The signal can be altered by tissue impedance, which means that a low velocity flow in a deep vessel will produce completely different PD patterns depending on the mother's abdominal wall thickness, the amount of amniotic fluid and the position of the foetus (Schulten-Wijman et al. 2011).
- The settings of the machine can sensibly modify the amount of signal registered by the processor, and therefore, the amount of colour voxels inside the VOI: the algorithms for refining the B-mode signal, like the speckle reduction or the cross beam reduction post-process algorithms, mask the signal processed and "erase" a significant amount of moving particles. (N J Raine-Fenning, Nordin, Ramnarine, Campbell, Clewes, Perkins & Johnson 2008b)
- The post-processing software provided by the developers of the Volume Measurement software: 4DView and virtual organ computer-aided analysis (VOCAL®) by General Electric Medical division. Q-lab® by Philips Medical Division, as well as Sonoview® and Histogram by Samsung-Medison Co show no correlation in their measurements. Therefore, the same structure, under similar circumstances, draw off different results once measurement of the VOI is performed. (J L Alcázar 2008)

2.1.1 The biases behind the algorithm

Based on previous observations, we conducted a preliminary study, on five healthy foetuses on their 20th week of gestation, comparing the values obtained in the same foetus with different machines and adjusting settings as main gain in 600 Hz, medium wall filter in 60 Hz, cross beam reduction off and persistence of colour signal in 0. In all of them the

structure was the Willis' polygon at the cranial base. Figure 5 shows the images obtained from the machines and the histograms.

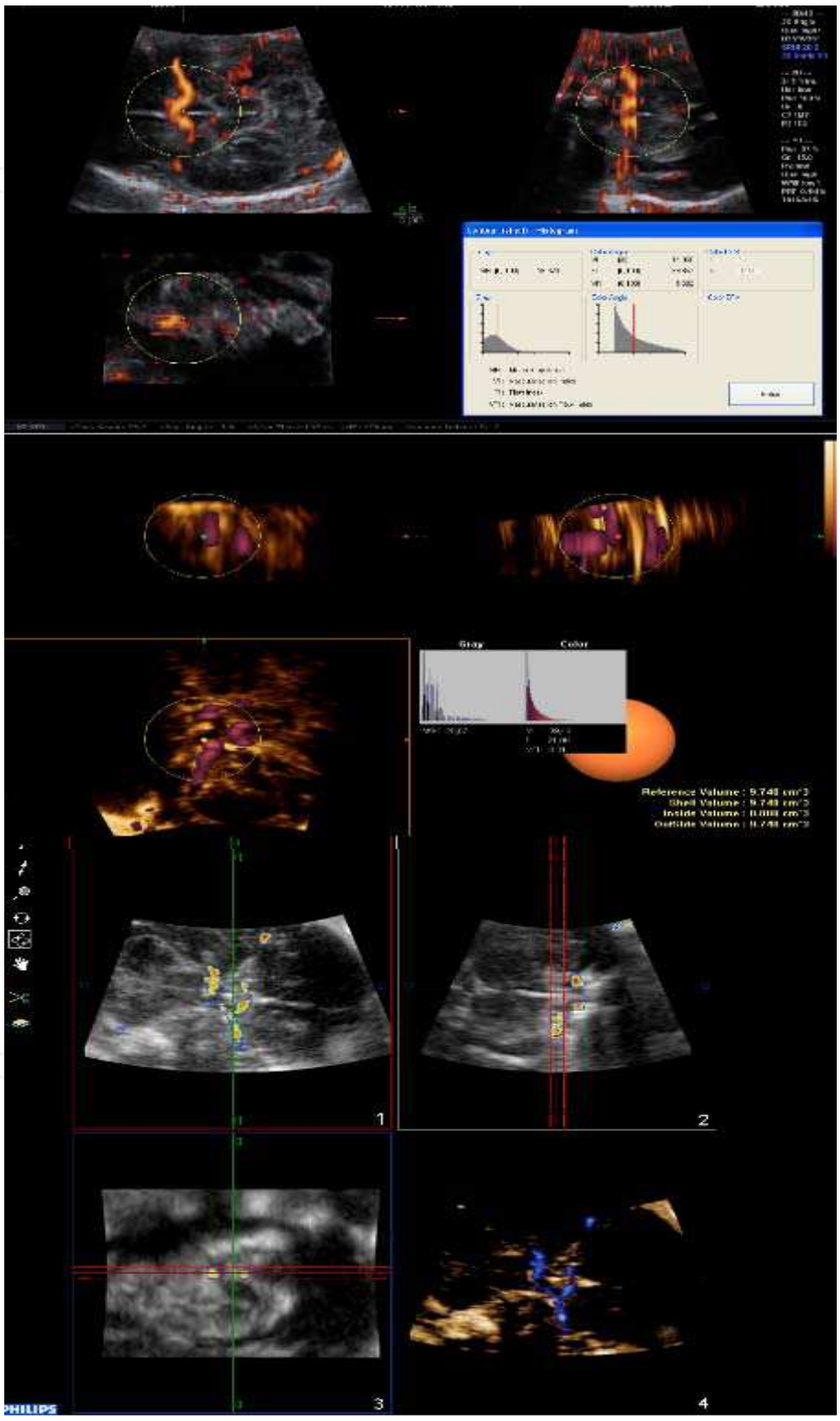


Fig. 5. Images obtained from a single foetus in cephalic presentation, from three different machines: General Electric Voluson E8 (Upper); Medison Accuvix V20 Prestige (Middle); Philips iU22 (Lower)

The results, summarized in the table 1, show how different the measurements are, depending on the brand. They also show how they differ among themselves, despite the same gestational age and similar maternal characteristics.

Foetus	GE Voluson E8			Philips iU22			Medison Accuvix V20		
	VI	FI	VFI	VI	FI	VFI	VI	FI	VFI
1	44.9	46.1	20.7	32.3	25..1	33.5	48.6	16.9	5.5
2	14.1	39.8	5.6	16.6	28.3	9.5	39.4	21.1	8.3
3	23.6	51.1	17.3	36.2	17.3	19.5	42.5	28.1	4.7
4	36.3	38.9	21.3	27.3	32.8	11.1	25.8	40.3	19.2
5	37.3	44.0	9.5	48.1	27.3	13.1	35.8	39.9	6.9

Table 1. Results from comparing similar VOI in three different machines, with the PD quantification application included in their software

In conclusion, normalizing the data from the 3D PD signal is currently not possible and reference ranges to discriminate normality from pathologic conditions are not available. Therefore, no feasibility for these indexes in obstetric clinical practice can be foreseen in the short term.

2.2 The regional normalization solution

Given that no decisions can be made from direct measurement of the abovementioned indexes, a possible approach could be to use two Regions of Interest (ROI) inside the same volume. The more reliable possibility after *in-vitro* testing was the VFI (N J Raine-Fenning, Nordin, Ramnarine, Campbell, Clewes, Perkins & Johnson 2008a). And the easier and more repeatable formula was a simple VFI index

$$VFI_1 / VFI_2 \tag{5}$$

2.2.1 The ductus venosus shunting as an example

In physiological conditions, few regions of foetal circulation can offer enough regional differences to be considered clinically relevant. But the most important of these is, no doubt, the physiological shunt in the ductus venosus which is not only a reliable indicator of preload, but also a sensitive mechanism of circulatory re-distribution in adverse circulatory conditions such as placental insufficiency (M Bellotti et al. 2000; Kiserud 2001).

The original description of Ductus Venosus Shunting (DVS) measurement was published by Belloti (Maria Bellotti et al. 2004), and was, simplifying, an index of estimated flow through Ductus Venosus (DV) over the one through Umbilical Vein (UV)

The classical way for estimating the flow through the UV is

$$Q_{UV} = 0.5 \times (V_{\max})_{UV} \times \pi \times (D_{UV}^2 / 4) \tag{6}$$

Where Vmax relates to the Umbilical Vein maximum velocity as measured by pulsed Doppler. 0,5 is a normalization constant related to foetal blood viscosity and DUV is the mean diameter of the umbilical vein in its abdominal portion.

Also, the calculation of DV flow, made by Belloti et al, is;

$$Q_{DV} = \left(-0.03 \times DR^2 + 0.189 \times DR + 0.43\right) \times (V_{\max})_{UV} \times \pi \times (D_{UV}^2 / 4) \quad (7)$$

Where Vmax DV is the maximum systolic velocity in the Ductus Venosus. DR respresents the ratio between the inlet (smaller) and the outlet (larger) of the ductus venosus, represented as part of a paraboloid equation

Therefore, the DVS could be expressed as

$$\left(Q_{DV} / Q_{UV}\right) \cdot \cdot 100 \quad (8)$$

A description of the ideal technique for measuring blood flow in both UV and DV has been published (Tchirikov et al. 2006). For UV blood volume flow measurement, a straight segment of the intra-abdominal part of the UV upstream of any hepatic branches should be selected, with the Doppler gate positioned so as to completely cover the vessel's diameter. The UV flow volume can also be measured in the umbilical cord. Authors suggest measuring blood flow volume following the 'maximum principle', which aims to determine the maximum diameter of the vessel, the maximum intensity weighted mean velocity (or time-averaged mean velocity, TAV) at the maximum vessel length in a straight longitudinal section. The inner vessel diameter is determined to the nearest tenth of a millimeter by placing the calipers at right angles to the vessel axis on a frozen B-mode image (without color). This is followed by the TAV measurement at the same vessel portion with a small insonation angle of insonation (less than 30°). The blood volume flow rate is calculated from diameter (D) and TAV as flow rate = TAV × π × (D/2)² mL/min. Regarding the DV, The inner diameter of the DV should be measured by insonating perpendicularly to the vessel wall at the isthmus. In order to reduce random error, the procedure must be repeated four or more times and the calculated mean diameter entered into the statistics (Kiserud et al. 2006). Doppler evaluations must be carried out in the absence of fetal breathing and body movements.

As it should become evident, the skills needed for achieving such measurements are prohibitively high; the time needed for every exploration is too long for a usual clinical exploration and the medical scope of this practice is quite reduced. Our proposal to address this issue is a far simpler, faster and repeatable approach, by using 3D PD. (Bello-Muñoz et al. 2009)

By taking a single volume of the foetal abdomen in Angio 3D PD mode, it was possible to measure the UV VFI by calculating it into a 1 cc sphere. After navigating through the volume, same measurement (DV VFI) was done in the DV, employing the same 1 cc sphere (Figure 6 summarizes both measurements)

Our study compared 162 volumes from normal foetuses and 36 from Foetal Growth Restriction (FGR) cases. In all of them we measured the DVS as described classically by Belloti et al (M Bellotti et al. 2007), and collected a volume of the foetal abdomen with 3D PD angio mode signal, always adjusting the same settings in the machine (General Electric Voluson E 8 GE Medical Systems Milwaukee USA) with a 3D RNA5-9-D Volume Convex Array Transducer Probe.

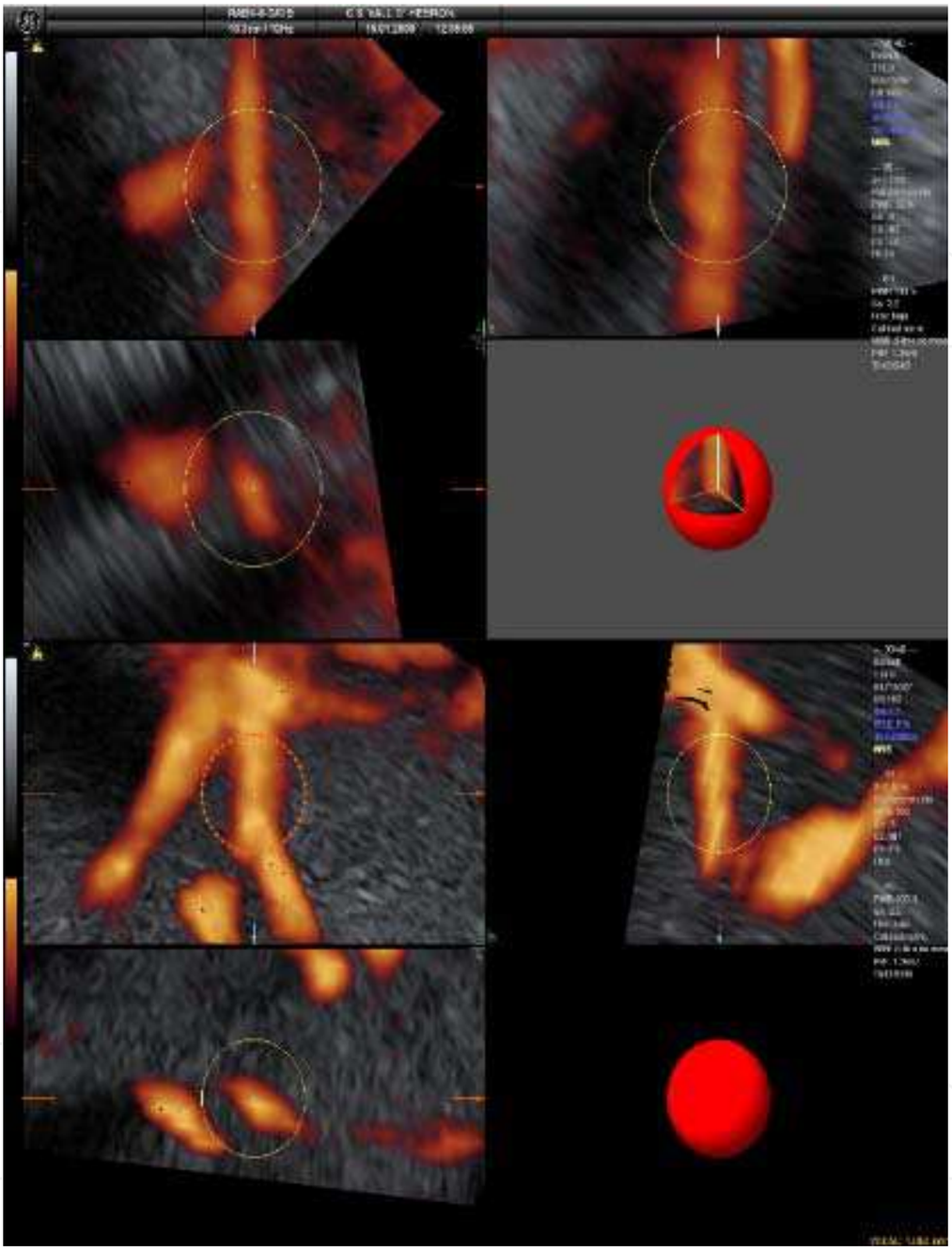


Fig. 6. VFI measurement in abdominal umbilical vein (upper) and in ductus venosus (lower). As the size of the sphere is exactly the same, the VOI remains unchanged

The calculation of the DV/UV VFI ratio was as simple as:

$$DV \cdot VFI \,/\, UV \cdot VFI. \cdot \cdot 100 \tag{9}$$

We found a significant positive correlation between DVS measured as described by Belloti et al and DVS measured as a ratio of DV/UV VFI (Figure 7)

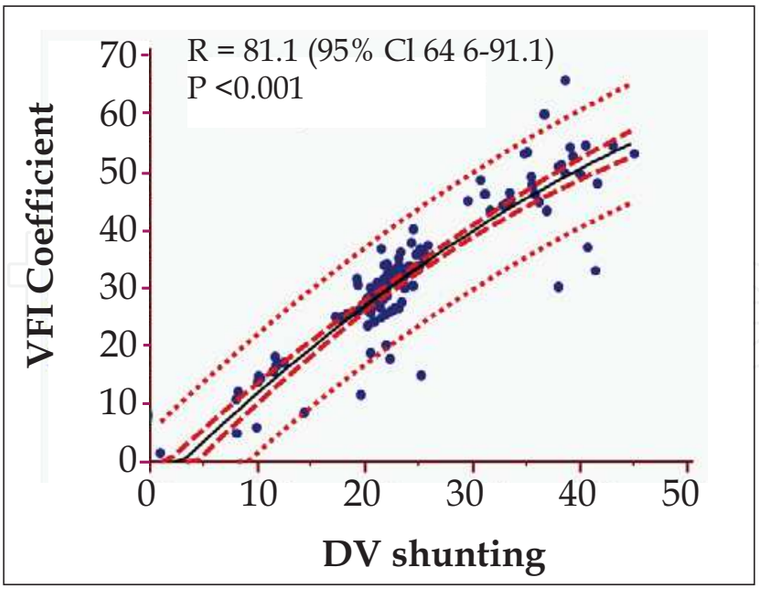


Fig. 7. Lineal regression plot comparing the DVS measured as classically described and the DV/UV VFI ratio r value = 0.81; P<0.001

Reference ranks equation $y = 0{,}6766 + 1{,}6542\ x + -0{,}007813\ x^2$

Also, as previously described, we found a significant difference in DV/UV VFI ratio between normal and FGR foetuses. Comparing results in growth restricted foetuses showed difference as plotted by gestational age mean (SD):39 (11,5) and 53(16,8) (p = 0,03). (Figure 8)

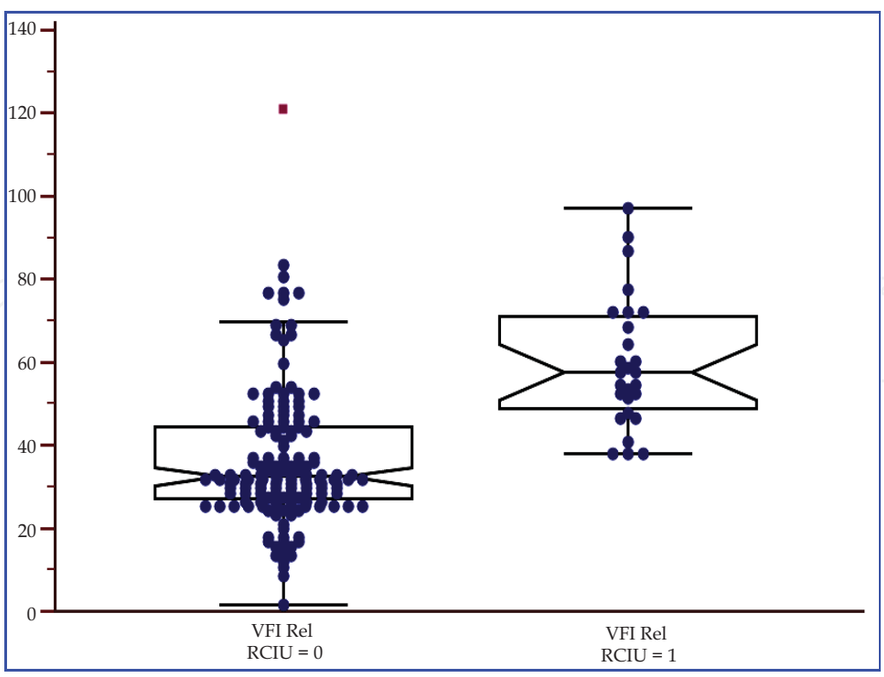


Fig. 8. Box Whisker plot of DV/UV VFI ratio comparing normal (left) to IUGR foetuses (right)

3. Four-dimensional power Doppler signal and the estimation of flow

3.1 The addition of a time sequence

Since the solution provided is already limited and only allows to estimate some regional changes in vascularity, applicable perhaps to the abovementioned DVS and to placenta (Odeh et al. 2011), but is still far away from depicting the flow phenomenon; it is necessary to move forward, towards two recently opened gates:

First is the integration of Power Doppler signal derived velocities profile, whose most reliable approach is the Surface Integration of Velocity Vectors, (Sun et al. 1995; J M Rubin et al. 2001; Berg et al. 2000) a clarifying concept which was developed for Color Dopler signal analysis, but has the handicap of the angle effect (Pemberton et al. 2005; Li et al. 2005), reason why it was left aside. Until the algorithms for calculating velocity of particles from power Doppler signals were developed (M. G. Jones et al. 2003; Kripfgans et al. 2006; Petersch & Hönigmann 2007)

Surface integration of velocity vectors is based on Gauss' theorem, which relates the divergence of the quantity (*v)* in an enclosed volume (*V)* to the flux through the surface (*S)* covering (*V)*. In other words, a surface integral of *v* over the enclosing boundary *S* will yield the volume flow *Q*:

$$Q = \int_S \vec{v} \cdot \overrightarrow{dA} \ . \tag{10}$$

The easiest way to implement SIVV is to choose a surface that is locally perpendicular to each Doppler beam. For this case, the right side dot product in Equation 1 will be replaced by a regular multiplication of the Doppler velocity and the size of the surface element. In other words, this surface has a constant depth geometry with respect to the Doppler beams. (Kripfgans et al. 2006)

The most general scanning geometry is the surface of a torus because the center of rotation for the axial-lateral and axial-elevational beams can differ). Volume flow can be computed by integrating all Doppler acquisitions on the defined surface, as expressed by Kripfgans et al:

$$Q = \sum_{i \in S} v_i a_i \tag{11}$$

Where, *Q* is the total flux through the surface *S*, which equals volume flow; *vi* is the local Doppler velocity; *ai* is the associated cross-sectional area on *S* for this voxel, and · is the dot product between the local velocity vector and the local surface normal. In this case, the detected velocity is parallel to the surface normal.

In Kripfgans et al experiment, for the depicted type of tube-to-transducer orientation, the left-/right-most Doppler beam has the smallest/largest Doppler angle, respectively. This causes the velocity maximum to shift toward the left. However, warping of velocity values does not affect the measured SIVV value. Inherent compensation of this warping is due to nonuniform distribution of surface elements over the tube cross section.

A very important matter, mainly derived from biophysical characteristics of blood is the Rouleaoux' effect (J M Rubin et al. 1997; A. W. Welsh et al. 2005; N J Raine-Fenning, Nordin,

Ramnarine, B. K. Campbell, Clewes, Perkins & Johnson 2008a). The local Doppler power is largest inside the vessel and smallest outside because of the effect of partial volume averaging and the Doppler wall filter effect, which gives the pixels inside the vessel a higher power. All Doppler data is wall filter processed internally in the scanner by the smallest setting possible on the machine. Therefore, it is mandatory to minimize filtering for the selected Doppler frequency range.

Authors define a solution for surface integration of velocity vectors, which was weighted on the basis of the Doppler power in the respective voxels. A velocity masking algorithm which was generated, using the Doppler power value *pT* to weight the velocity values of the integration surface.

Therefore, the modified SIVV method that was used by the authors was

$$Q = \sum_{i \in S} (v_i \cdot a_i) p_i \ . \tag{12}$$

Where, *pi* is a scaling factor based on the local Doppler power. Power weighting factors *pi* were set to 1 for all Doppler powers larger then *pT*. Values between 0 and *pT* were scaled between 0 and 1 on the basis of their Doppler power value. The justification for the selection/scaling process is that voxels near the wall, which partially contain flow and soft tissue, will show lower than- maximum Doppler power. Fractional power is therefore weighted by fractional scaling factors. So far, the threshold *pTwas* set empirically by developers. However, it was set constant for all measurements, and it could be shown that the *pT* contour fills the lumen. User-selected Doppler gain was adjusted as needed to compensate for signal reduction due to large angles between flow and Doppler beams.

The next addition to the conceptual framework was the estimation of pulsatile conditions by Richards and Kripfgans (Richards et al. 2009), by adding to the model the potential signal fluctuations derived from the wall movements and the local velocity profile changes derived from particles acceleration. As a first issue, authors defined the possibility of collecting not one, but *N* number of velocity profiles according to the local variations in time and position. Such local velocities were expressed as:

$$\widehat{v_i} = E\left(v_i\left(X_i\right)\right) = \frac{\sum_{j=1}^{N} v\left(X_i, t_j\right)}{N}, \tag{13}$$

Where $E(vi(Xi))$ is the expected value of the local velocity estimates. $v(Xi,tj)$ are the local velocity estimates that are measured at randomly selected time increments defined by t*j* as follows:

$$t_{j+1} = t_j + t_s + t_r, \tag{14}$$

Authors defined an experiment to obtain the average volume flow in the presence of pulsatility: 50 random time points distributed across the equivalent of a cardiac cycle were collected and averaged at each location. Power Doppler data were then used to correct for partial volume effects as described in the previous paragraph. Then, using seven previously defined surfaces for flow estimate, the equation for the modified SIVV method, became:

$$Q = \frac{1}{M} \sum_{i \in S_M} s_i \bullet w_i \bullet \widehat{v_i} \ , \tag{15}$$

where *M* is the number of integration surfaces and the surface of integration *(S)* has been modified to include the *M* surfaces *(SM)*.

In our opinion, Richards & Kripfgans' works have achieved a breakthrough in this matter, and the experiment we have developed is nothing but a logical consequence of their postulations.

Before describing the experiment, next consequent step was to add a regular time frame to the algorithm. Fortunately, the tool for getting the initial data was already developed and seated on the machine: The Spatio Temporal Image Correlation (STIC) is an automated volume acquisition in which the array inside the transducer housing performs a slow, single sweep, recording one single 3D data set. This volume consists of a high number of 2D frames, one behind the other. Due to the small region of interest required to image the foetal heart, the B-mode frame rate during the acquisition of the volume scan is very high, in the range of 150 frames/s. Assuming a volume acquisition time of 10 s and sweeping over an area of 25° (both parameters can be adjusted), there are 1500 B-mode images in the volume memory. During this acquisition time the fetal heart beats 20–25 times, which means there are 20–25 images showing a systolic peak contained within these 1500 B-mode frames (DeVore et al. 2003; Chaoui & Heling 2005). Concerning this application, further studies have shown how, the mere analysis of intra-ventricular stroke volume in left and right heart gave information reliable enough for calculating the cardiac output in foetuses from 16 to 32 weeks (Molina, Faro, Sotiriadis, Dagklis & Nicolaides 2008a).

Basis of volume calculation in VOCAL are performed by integration of polygon areas marked in parallel planes. The method used for the integration of the polygon areas is given by the formula

$$Vol - \frac{\pi}{N} \cdot \left[\sum_{i=1}^{2 \cdot N} TA_i \cdot ds_i \right] \tag{16}$$

Where N = number of marked polygon areas Ai = polygon area in plane i di,j = distance between plane i and plane j the sort order of planes 1,..., N is given by d1,2 £ d1,3 £... £ d1,N. (Sohn 1993; Robb et al. 1997).

And the basis for stroke volume calculation and cardiac output calculation were (Molina, Faro, Sotiriadis, Dagklis & Nicolaides 2008b):

$$CO = \lim_{n \to \infty} \left(1 + \frac{1}{n} \right)^n \cdot Vs \ \vdots - \vdots \ \lim_{n \to \infty} \left(1 + \frac{1}{n} \right)^n \cdot VD \tag{17}$$

Where CO = Cardiac Output, VS is Systolic Volume and VD is Diastolic Volume.

The abovementioned approach provides some additional information on cardiac output and has proven to be repeatable and more accurate than previous methods (Messing et al. 2007; Hamill et al. 2011; Simioni et al. 2011). Notwithstanding, it still has a substantial amount of human interaction, and is rather time-consuming as for being used in an actual clinical setting.

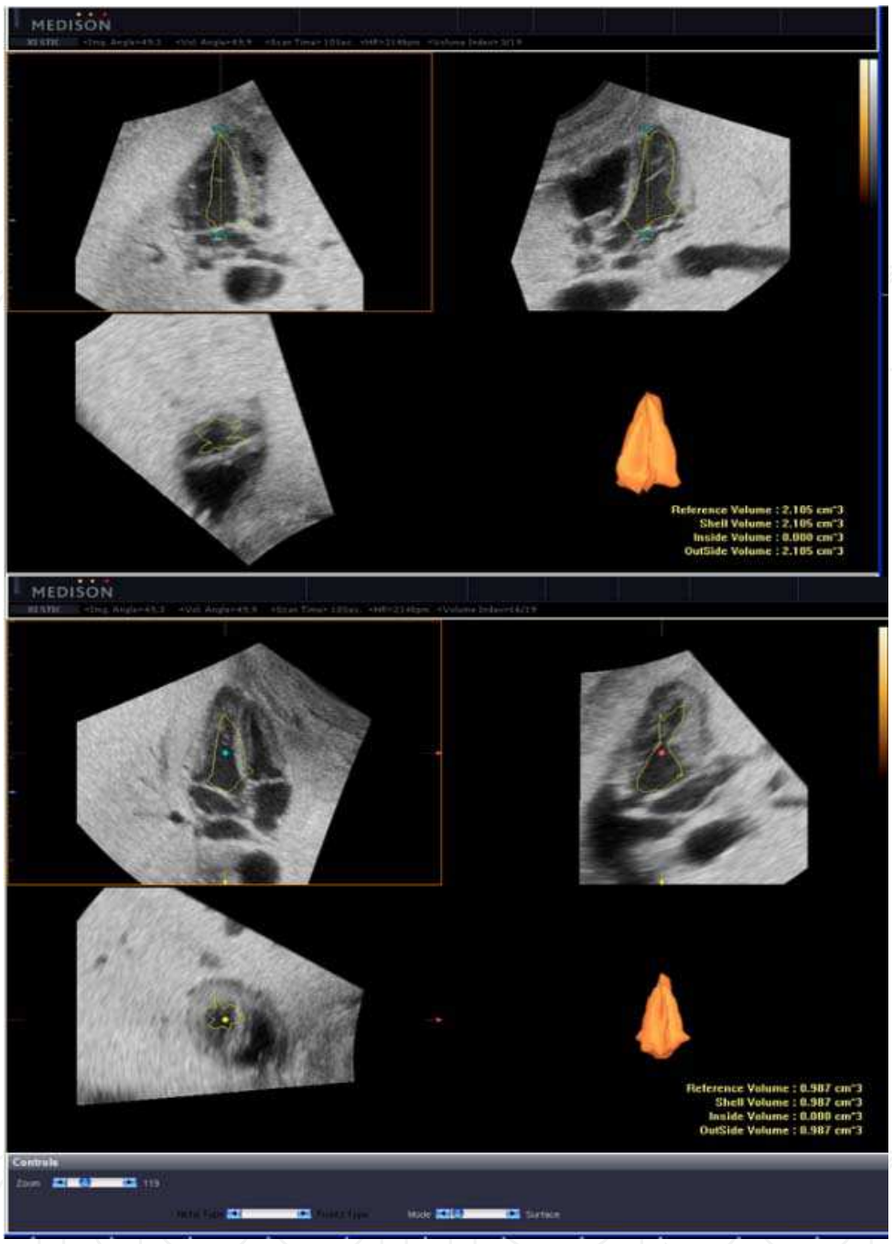


Fig. 9. Reproduction of STIC and VOCAL model for left ventricle output calculation in a term ovine foetus, taken by the authors during their experiment (Bello-Muñoz et al. 2010); as proposed by Molina et al.

3.1.1 The cardiac output model

Based on previous studies and encouraged by the works of Richards & Kripfgans, we decided to develop an algorithm of flow calculation, based on surface integration of velocity vectors and time frame sequences from STIC volumes. Volume datasets as obtained by the ultrasound machine Medison Accuvix V-20 prestige with a Medison 3D4-8ET 3D volumetric probe (Samsung Medical Co, Hoofddorp, Nz).

A total of eight foetuses from near term pregnant sheep (125-140 days) were exteriorized through a cesarean section and a modified central catheter inserted via umbilical cord and under direct echographic vision. An arterial line was also inserted in one of the umbilical arteries. Both transducers from the catheters were connected to a PICCO monitor for invasive testing (PULSION Medical Inc. Irving TX, USA). Continuous measurement of combined cardiac output was the registered as long as the experiment was carried out, meanwhile one of the authors (JB-M), recorded several volume datasets synchronizing the register of the data set with data obtained by monitorization. Analysis of all the data was made offline.

A complete spreadsheet of physiologic registers from the experimental subject was recorded for comparison and external validation of calculations. All images were processed by using the Mathematica® software (Wolfram Research Europe Ltd., Oxfordshire, UK). All data from VOI analysis was addded to the calculation spreadsheet and a polinomial regression fit model was designed

The mathematical background of this study was based on flow calculation:

$$Q = \sum_{i \in S} (\nu_i \cdot a_i) p_i \ . \tag{12}$$

And the concept of vector velocity profile described above. But with the addition of a time frame provided by the STIC algorithm, which means a continuous sum of velocity profiles, giving us a new profile of the area, represented as:

$$(1+A)^n = 1 + \frac{Ax}{1!} + \frac{A(n-1)x^2}{2!} + \cdots \tag{18}$$

And to the velocity profile, expressed also as

$$\sum \ vi(t1) + vi(t2) \ldots \ \ldots vi()tn \tag{19}$$

Where N is the entire amount of frames included in a cardiac cycle.

Once collected the sequences, information of velocity vector profile (VVP) form the VOI was collected in a series of frames, from the starting of the cardiac cycle (early start of diastole), denominated as t_0 until the end of same cycle (end of systole) hence called t_n. Information of VVP was then modified according to area variation in every frame. Therefore, the mathematical expression of this phenomenon could be expressed as a matrix of data:

$$\begin{aligned} \sum_{t=1}^{N} Qn = \big(& (A1.vi1)t1 \vdots (A2.vi2)t1 \vdots \cdots \vdots (Ax.vix)t1 \vdots (A1.vi1)t2 \vdots (A2.vi2)t2 \vdots \cdots \vdots \\ & (Ax.vix)t2 \vdots (A1.vi1)tn \vdots (A2.vi2)tn \vdots \cdots \vdots (Ax.vix)tn \big) \end{aligned} \tag{20}$$

Where A_x is an estimated area obtained by adding all the regional areas in the VOI and vi_x is the velocity vector profile in each sub-area, according to, previously described, sectorial variations in velocity. And t is the timeline described above.

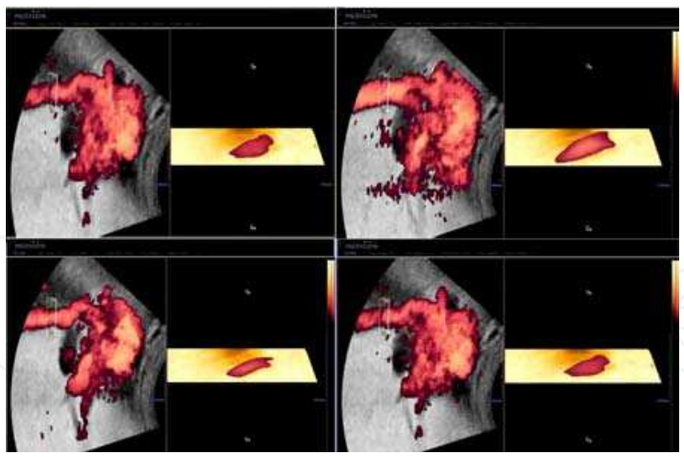


Fig. 10. Screen snapshot of descending aorta plane with selected volume of evaluation. Right side of the image is the VOI containing the $v_1 \ldots v_n$ information. A set of voxels like this one was added to the matrix, since t_1 till t_n where n=end of the cardiac cycle. (Actual experiment added measurements from the aortic isthmus, this image is for illustrative purposes)

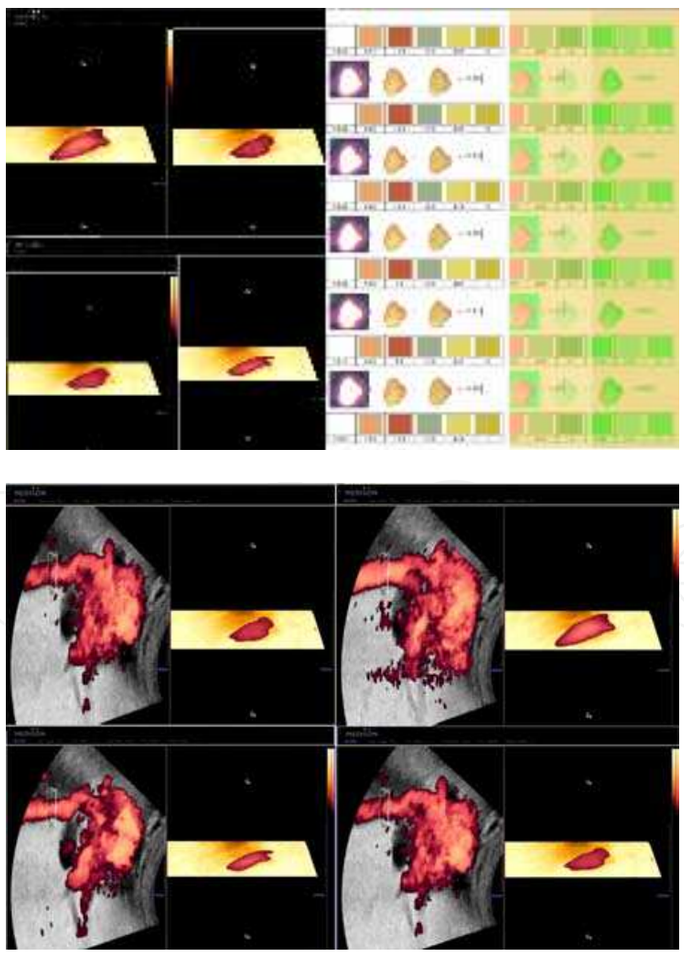


Fig. 11. Colour deconvolution algorithm as delivered by the Mathematica software ®

Regression analysis showed a strong correlation between actual measurement of Combined cardiac Output as obtained by invasive methods and the estimated flow 4D PD dataset as calculated by the authors. The reference polynomial equation and plot is showed in Figure 11

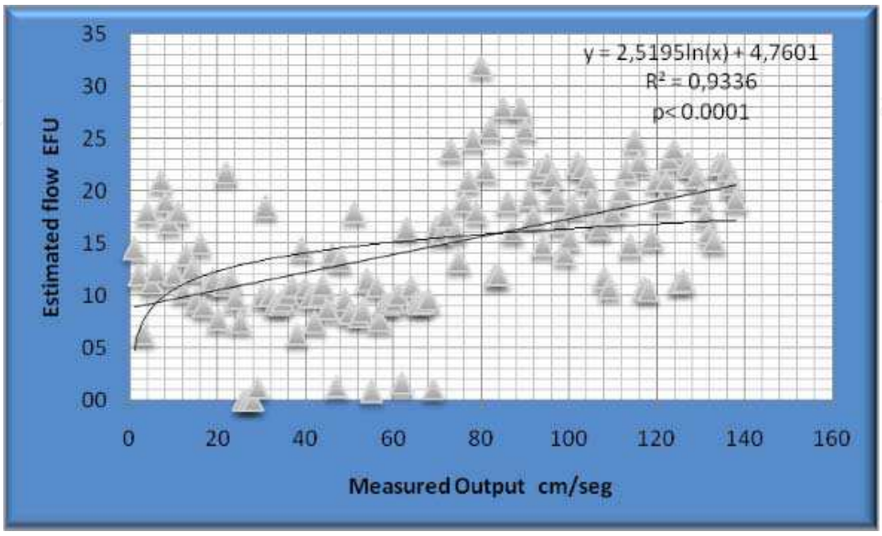


Fig. 12. Polinomial regression plot

4. Conclusion

Three dimensional power Doppler (3D PD), in its current state has no correlation with actual flow measurements, since there is no way of involving the time as a magnitude. Four dimensional power Doppler, by adding the surface integration of velocity vectors from power Doppler signal, and the Spatio Time Image correlation (STIC) might improve significantly its potential. An important amount of additional research on this field is mandatory in order to grant its utility in clinical conditions. But 4D PD could be, in the near future, the most reliable tool for non invasive assessment of physiological intrauterine magnitudes, as Cardiac Output, vascular shunting and flow variations, in normal as well as in pathological conditions

5. Acknowledgment

The authors wish to thank Drs Marielle Estevez and Carla Fonseca from the animal house of the Institut de Recerca de l'Hospital Universitari Vall d'Hebron for their invaluable help in animal care and preparation. They also wish to express their gratitude to Dr Jose Lluis Peiró for his surgical intervention on the mother sheep and the instrumentation of foetuses as well as for his generous teaching and support.

6. References

Alcázar, J L, 2008. Three-dimensional power Doppler derived vascular indices: what are we measuring and how are we doing it? Ultrasound in Obstetrics & Gynecology: The

Official Journal of the International Society of Ultrasound in Obstetrics and Gynecology, 32(4), págs.485-487.

Alcázar, Juan Luis & Jurado, M., 2011. Three-dimensional ultrasound for assessing women with gynecological cancer: a systematic review. Gynecologic Oncology, 120(3), págs.340-346.

Bello-Muñoz, J. et al., 2009. OP23.05: A three-dimensional power Doppler algorithm for ductus venosus shunting evaluation in normal and growth restricted fetuses. Ultrasound in Obstetrics & Gynecology, 34(S1), págs.136-137.

Bellotti, M, Pennati, G. & Ferrazzi, E., 2007. Re: ductus venosus shunting in growth-restricted fetuses and the effect of umbilical circulatory compromise. Ultrasound in Obstetrics & Gynecology: The Official Journal of the International Society of Ultrasound in Obstetrics and Gynecology, 29(1), págs.100-101; author reply 101-102.

Bellotti, M et al., 2000. Role of ductus venosus in distribution of umbilical blood flow in human fetuses during second half of pregnancy. American Journal of Physiology. Heart and Circulatory Physiology, 279(3), págs.H1256-1263.

Bellotti, Maria et al., 2004. Simultaneous measurements of umbilical venous, fetal hepatic, and ductus venosus blood flow in growth-restricted human fetuses. American Journal of Obstetrics and Gynecology, 190(5), págs.1347-1358.

Bendick, P.J. et al., 1998. Three-dimensional vascular imaging using Doppler ultrasound. American Journal of Surgery, 176(2), págs.183-187.

Berg, S. et al., 2000. Volumetric blood flow measurement with the use of dynamic 3-dimensional ultrasound color flow imaging. Journal of the American Society of Echocardiography: Official Publication of the American Society of Echocardiography, 13(5), págs.393-402.

Bozkurt, N., Başgül Yigiter, A., et al., 2010. Correlations of fetal-maternal outcomes and first trimester 3-D placental volume/3-D power Doppler calculations. Clinical and Experimental Obstetrics & Gynecology, 37(1), págs.26-28.

Burns, P.N., 1992. Measuring volume flow with Doppler ultrasound-an old nut. Ultrasound in Obstetrics & Gynecology: The Official Journal of the International Society of Ultrasound in Obstetrics and Gynecology, 2(4), págs.238-241.

Cruz-Martinez, R et al., 2011. Normal reference ranges of fetal regional cerebral blood perfusion as measured by fractional moving blood volume. Ultrasound in Obstetrics & Gynecology: The Official Journal of the International Society of Ultrasound in Obstetrics and Gynecology, 37(2), págs.196-201.

Cruz-Martinez, Rogelio et al., 2009. Cerebral blood perfusion and neurobehavioral performance in full-term small-for-gestational-age fetuses. American Journal of Obstetrics and Gynecology, 201(5), págs.474.e1-7.

Chang, C.-H. et al., 2003. Assessment of normal fetal liver blood flow using quantitative three-dimensional power Doppler ultrasound. Ultrasound in Medicine & Biology, 29(7), págs.943-949.

Chaoui, R. & Heling, K.S., 2005. New developments in fetal heart scanning: three- and four-dimensional fetal echocardiography. Seminars in Fetal & Neonatal Medicine, 10(6), págs.567-577.

Chaoui, R. & Kalache, K.D., 2001. Three-dimensional power Doppler ultrasound of the fetal great vessels. Ultrasound in Obstetrics & Gynecology: The Official Journal of the

International Society of Ultrasound in Obstetrics and Gynecology, 17(5), págs.455-456.

Dar, P. et al., 2010. First-trimester 3-dimensional power Doppler of the uteroplacental circulation space: a potential screening method for preeclampsia. American Journal of Obstetrics and Gynecology, 203(3), págs.238.e1-7.

DeVore, G.R. et al., 2003. Spatio-temporal image correlation (STIC): new technology for evaluation of the fetal heart. Ultrasound in Obstetrics & Gynecology: The Official Journal of the International Society of Ultrasound in Obstetrics and Gynecology, 22(4), págs.380-387.

Dubiel, M. et al., 2005. Computer analysis of three-dimensional power angiography images of foetal cerebral, lung and placental circulation in normal and high-risk pregnancy. Ultrasound in Medicine & Biology, 31(3), págs.321-327.

Eik-Nes, S.H. et al., 1982. Ultrasonic measurement of human fetal blood flow. Journal of Biomedical Engineering, 4(1), págs.28-36.

Fenster, A., Lee, D., et al., 1998. Three-dimensional ultrasound imaging of the vasculature. Ultrasonics, 36(1-5), págs.629-633.

Forsberg, F. et al., 1995. Volume flow estimation using time domain correlation and ultrasonic flowmetry. Ultrasound in Medicine & Biology, 21(8), págs.1037-1045.

Gill, R.W., 1979. Pulsed Doppler with B-mode imaging for quantitative blood flow measurement. Ultrasound in Medicine & Biology, 5(3), págs.223-235.

Guimarães Filho, H.A. et al., 2011. Reproducibility of three-dimensional power Doppler placental vascular indices in pregnancies between 26 and 35 weeks. Archives of Gynecology and Obstetrics, 283(2), págs.213-217.

Guo, Z. & Fenster, A., 1996. Three-dimensional power Doppler imaging: a phantom study to quantify vessel stenosis. Ultrasound in Medicine & Biology, 22(8), págs.1059-1069.

Guo, Z., Durand, L.G., et al., 1998. In vitro evaluation of multiple arterial stenoses using three-dimensional power Doppler angiography. Journal of Vascular Surgery: Official Publication, the Society for Vascular Surgery [and] International Society for Cardiovascular Surgery, North American Chapter, 27(4), págs.681-688.

Harrington, K., Deane, C. & Campbell, S., 1996. Measurement of volume flow with time domain and M-mode imaging: in vitro and in vivo validation studies. Journal of Ultrasound in Medicine: Official Journal of the American Institute of Ultrasound in Medicine, 15(10), págs.715-720.

Hayashi, T. et al., 1998. Three-dimensional reconstruction of the power flow Doppler imaging of intracranial vascular structures in the neonate. Journal of Neuroimaging: Official Journal of the American Society of Neuroimaging, 8(2), págs.94-96.

Heling, K.S., Chaoui, R. & Bollmann, R., 2000. Prenatal depiction of the angioarchitecture of an aneurysm of the vein of Galen with three-dimensional color power angiography. Ultrasound in Obstetrics & Gynecology: The Official Journal of the International Society of Ultrasound in Obstetrics and Gynecology, 15(4), pág.345.

Hernandez-Andrade, E et al., 2008. Changes in regional fetal cerebral blood flow perfusion in relation to hemodynamic deterioration in severely growth-restricted fetuses. Ultrasound in Obstetrics & Gynecology: The Official Journal of the International Society of Ultrasound in Obstetrics and Gynecology, 32(1), págs.71-76.

Hernandez-Andrade, E, Jansson, T, et al., 2004. Validation of fractional moving blood volume measurement with power Doppler ultrasound in an experimental sheep model. Ultrasound in Obstetrics & Gynecology: The Official Journal of the International Society of Ultrasound in Obstetrics and Gynecology, 23(4), págs.363-368.

Hernandez-Andrade, E, Thuring-Jönsson, A., et al., 2004. Fractional moving blood volume estimation in the fetal lung using power Doppler ultrasound: a reproducibility study. Ultrasound in Obstetrics & Gynecology: The Official Journal of the International Society of Ultrasound in Obstetrics and Gynecology, 23(4), págs.369-373.

Jansson, Tomas et al., 2003. Estimation of fractional moving blood volume in fetal lung using Power Doppler ultrasound, methodological aspects. Ultrasound in Medicine & Biology, 29(11), págs.1551-1559.

Jones, M.G., Shipley, J.A. & Robinson, T.M., 2003. Visualisation of 4-D colour and power Doppler data. Ultrasound in Medicine & Biology, 29(12), págs.1735-1747.

Jones, N.W. et al., 2011. Evaluating the intra- and interobserver reliability of three-dimensional ultrasound and power Doppler angiography (3D-PDA) for assessment of placental volume and vascularity in the second trimester of pregnancy. Ultrasound in Medicine & Biology, 37(3), págs.376-385.

Kiserud, T., 2001. The ductus venosus. Seminars in Perinatology, 25(1), págs.11-20.

Kiserud, T. et al., 2006. Ductus venosus shunting in growth-restricted fetuses and the effect of umbilical circulatory compromise. Ultrasound in Obstetrics & Gynecology: The Official Journal of the International Society of Ultrasound in Obstetrics and Gynecology, 28(2), págs.143-149.

Kripfgans, O.D. et al., 2006. Measurement of volumetric flow. Journal of Ultrasound in Medicine: Official Journal of the American Institute of Ultrasound in Medicine, 25(10), págs.1305-1311.

Kupesic, S. & Kurjak, A., 2000. Contrast-enhanced, three-dimensional power Doppler sonography for differentiation of adnexal masses. Obstetrics and Gynecology, 96(3), págs.452-458.

Kurjak, A. et al., 1998. The assessment of ovarian tumor angiogenesis: what does three-dimensional power Doppler add? Ultrasound in Obstetrics & Gynecology: The Official Journal of the International Society of Ultrasound in Obstetrics and Gynecology, 12(2), págs.136-146.

Lai, P.K., Wang, Y.A. & Welsh, A.W., 2010. Reproducibility of regional placental vascularity/perfusion measurement using 3D power Doppler. Ultrasound in Obstetrics & Gynecology: The Official Journal of the International Society of Ultrasound in Obstetrics and Gynecology, 36(2), págs.202-209.

Li, X. et al., 2005. A novel method for the assessment of the accuracy of computing laminar flow stroke volumes using a real-time 3D ultrasound system: In vitro studies. European Journal of Echocardiography: The Journal of the Working Group on Echocardiography of the European Society of Cardiology, 6(6), págs.396-404.

Marín, R.C. et al., 2010. Use of 3-dimensional sonography for prenatal evaluation and follow-up of fetal goitrous hypothyroidism. Journal of Ultrasound in Medicine: Official Journal of the American Institute of Ultrasound in Medicine, 29(9), págs.1339-1343.

Martins, W.P. & Raine-Fenning, N J, 2010. Analysis and acquisition reproducibility of 3D power Doppler. Ultrasound in Obstetrics & Gynecology: The Official Journal of the International Society of Ultrasound in Obstetrics and Gynecology, 36(3), págs.392-393; author reply 393-394.

Morel, O. et al., 2010. Correlation between uteroplacental three-dimensional power Doppler indices and true uterine blood flow: evaluation in a pregnant sheep model. Ultrasound in Obstetrics & Gynecology: The Official Journal of the International Society of Ultrasound in Obstetrics and Gynecology, 36(5), págs.635-640.

Moskalik, A.P. et al., 2001. Analysis of three-dimensional Doppler ultrasonographic quantitative measures for the discrimination of prostate cancer. Journal of Ultrasound in Medicine: Official Journal of the American Institute of Ultrasound in Medicine, 20(7), págs.713-722.

Nardozza, L.M.M. et al., 2009. Evolution of 3-D power Doppler indices of fetal brain in normal pregnancy. Ultrasound in Medicine & Biology, 35(4), págs.545-549.

Negrini, R. et al., 2011. Assessment of placental blood flow between 22 and 34 weeks of gestation by 3D-sonography power Doppler vascular indices. Archives of Gynecology and Obstetrics, 284(1), págs.53-57.

Odeh, M. et al., 2011. Placental volume and three-dimensional power Doppler analysis in prediction of pre-eclampsia and small for gestational age between Week 11 and 13 weeks and 6 days of gestation. Prenatal Diagnosis, 31(4), págs.367-371.

Odibo, A.O. et al., 2011. Placental volume and vascular flow assessed by 3D power Doppler and adverse pregnancy outcomes. Placenta, 32(3), págs.230-234.

Pairleitner, H. et al., 1999. Three-dimensional power Doppler sonography: imaging and quantifying blood flow and vascularization. Ultrasound in Obstetrics & Gynecology: The Official Journal of the International Society of Ultrasound in Obstetrics and Gynecology, 14(2), págs.139-143.

Pemberton, J. et al., 2005. The use of live three-dimensional Doppler echocardiography in the measurement of cardiac output: an in vivo animal study. Journal of the American College of Cardiology, 45(3), págs.433-438.

Petersch, B. & Hönigmann, D., 2007. Blood flow in its context: combining 3D B-mode and color Doppler ultrasonic data. IEEE Transactions on Visualization and Computer Graphics, 13(4), págs.748-757.

Pomorski, M. et al., 2011. Comparative analysis of placental vasculature and placental volume in normal and IUGR pregnancies with the use of three-dimensional Power Doppler. Archives of Gynecology and Obstetrics. Available at: http://www.ncbi.nlm.nih.gov/pubmed/21744006 [Accedido Julio 17, 2011].

Raine-Fenning, N J, Nordin, N.M., Ramnarine, K.V., Campbell, B.K., Clewes, J.S., Perkins, A. & Johnson, I.R., 2008a. Determining the relationship between three-dimensional power Doppler data and true blood flow characteristics: an in-vitro flow phantom experiment. Ultrasound in Obstetrics & Gynecology: The Official Journal of the International Society of Ultrasound in Obstetrics and Gynecology, 32(4), págs.540-550.

Raine-Fenning, N J, Nordin, N.M., Ramnarine, K.V., Campbell, B.K., Clewes, J.S., Perkins, A. & Johnson, I.R., 2008b. Evaluation of the effect of machine settings on quantitative three-dimensional power Doppler angiography: an in-vitro flow phantom experiment. Ultrasound in Obstetrics & Gynecology: The Official Journal of the

International Society of Ultrasound in Obstetrics and Gynecology, 32(4), págs.551-559.

Richards, M.S. et al., 2009. Mean volume flow estimation in pulsatile flow conditions. Ultrasound in Medicine & Biology, 35(11), págs.1880-1891.

Rizzo, G. et al., 2009. First-trimester placental volume and vascularization measured by 3-dimensional power Doppler sonography in pregnancies with low serum pregnancy-associated plasma protein a levels. Journal of Ultrasound in Medicine: Official Journal of the American Institute of Ultrasound in Medicine, 28(12), págs.1615-1622.

Ruano, R. et al., 2006. Quantitative analysis of fetal pulmonary vasculature by 3-dimensional power Doppler ultrasonography in isolated congenital diaphragmatic hernia. American Journal of Obstetrics and Gynecology, 195(6), págs.1720-1728.

Rubin, J M, 1999. Flow quantification. European Radiology, 9 Suppl 3, págs.S368-371.

Rubin, J M et al., 1994. Power Doppler US: a potentially useful alternative to mean frequency-based color Doppler US. Radiology, 190(3), págs.853-856.

Rubin, J M et al., 1997. Normalizing fractional moving blood volume estimates with power Doppler US: defining a stable intravascular point with the cumulative power distribution function. Radiology, 205(3), págs.757-765.

Rubin, J M, Tuthill, T.A. & Fowlkes, J B, 2001. Volume flow measurement using Doppler and grey-scale decorrelation. Ultrasound in Medicine & Biology, 27(1), págs.101-109.

Sauders, J.B., Wright, N. & Lewis, K.O., 1980. Measurement of human fetal blood flow. British Medical Journal, 280(6210), págs.283-284.

Schulten-Wijman, M.J. et al., 2011. Re: Three-dimensional power Doppler: validity and reliability. Ultrasound in Obstetrics & Gynecology: The Official Journal of the International Society of Ultrasound in Obstetrics and Gynecology, 37(5), págs.620-621.

Sun, Y. et al., 1995. Estimation of volume flow rate by surface integration of velocity vectors from color Doppler images. Journal of the American Society of Echocardiography: Official Publication of the American Society of Echocardiography, 8(6), págs.904-914.

Tchirikov, M., Schröder, H.J. & Hecher, K., 2006. Ductus venosus shunting in the fetal venous circulation: regulatory mechanisms, diagnostic methods and medical importance. Ultrasound in Obstetrics & Gynecology: The Official Journal of the International Society of Ultrasound in Obstetrics and Gynecology, 27(4), págs.452-461.

Tuuli, M.G. et al., 2010. Validation of placental vascular sonobiopsy for obtaining representative placental vascular indices by three-dimensional power Doppler ultrasonography. Placenta, 31(3), págs.192-196.

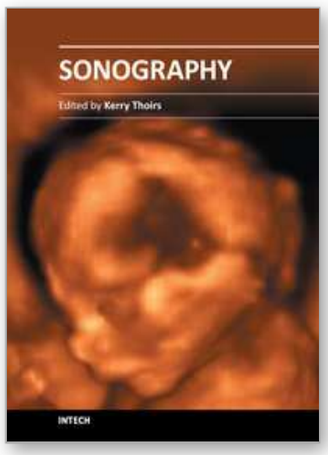
Welsh, A., 2004. Quantification of power Doppler and the index «fractional moving blood volume» (FMBV). Ultrasound in Obstetrics & Gynecology: The Official Journal of the International Society of Ultrasound in Obstetrics and Gynecology, 23(4), págs.323-326.

Welsh, A.W. et al., 2005. Standardization of power Doppler quantification of blood flow in the human fetus using the aorta and inferior vena cava. Ultrasound in Obstetrics & Gynecology: The Official Journal of the International Society of Ultrasound in Obstetrics and Gynecology, 26(1), págs.33-43.

Yigiter, A.B. et al., 2011. Placental volume and vascularization flow indices by 3D power Doppler US using VOCAL technique and correlation with IGF-1, free beta-hCG, PAPP-A, and uterine artery Doppler at 11-14 weeks of pregnancy. Journal of Perinatal Medicine, 39(2), págs.137-141.

IntechOpen

IntechOpen



Sonography

Edited by Dr. Kerry Thoirs

ISBN 978-953-307-947-9
Hard cover, 346 pages
Publisher InTech
Published online 03, February, 2012
Published in print edition February, 2012

Medical sonography is a medical imaging modality used across many medical disciplines. Its use is growing, probably due to its relative low cost and easy accessibility. There are now many high quality ultrasound imaging systems available that are easily transportable, making it a diagnostic tool amenable for bedside and office scanning. This book includes applications of sonography that can be used across a number of medical disciplines including radiology, thoracic medicine, urology, rheumatology, obstetrics and fetal medicine and neurology. The book revisits established applications in medical sonography such as biliary, testicular and breast sonography and sonography in early pregnancy, and also outlines some interesting new and advanced applications of sonography.

How to reference

In order to correctly reference this scholarly work, feel free to copy and paste the following:

Juan Carlos Bello-Munoz, Mauricio Ayala, Elena Carreras, Paula Oliveros, Nazareth Campo, Alexandra Casasbuenas, Silvia Arévalo and Lluis Cabero (2012). Future Uses of Three/Four Dimensional Power Doppler Signal in Fetal Medicine, Sonography, Dr. Kerry Thoirs (Ed.), ISBN: 978-953-307-947-9, InTech, Available from: http://www.intechopen.com/books/sonography/future-uses-of-three-four-dimensional-power-doppler-signal-in-fetal-medicine

INTECH
open science | open minds

InTech Europe
University Campus STeP Ri
Slavka Krautzeka 83/A
51000 Rijeka, Croatia
Phone: +385 (51) 770 447
Fax: +385 (51) 686 166
www.intechopen.com

InTech China
Unit 405, Office Block, Hotel Equatorial Shanghai
No.65, Yan An Road (West), Shanghai, 200040, China
中国上海市延安西路65号上海国际贵都大饭店办公楼405单元
Phone: +86-21-62489820
Fax: +86-21-62489821

© 2012 The Author(s). Licensee IntechOpen. This is an open access article distributed under the terms of the Creative Commons Attribution 3.0 License, which permits unrestricted use, distribution, and reproduction in any medium, provided the original work is properly cited.

IntechOpen

IntechOpen